Journal of Solid State Chemistry 237 (2016) 269–273

Contents lists available at ScienceDirect

Journal of Solid State Chemistry

journal homepage: www.elsevier.com/locate/jssc

Thermal properties and phase transition in the fluoride, $(NH_4)_3SnF_7$

A.V. Kartashev [a,b], M.V. Gorev [a,c], E.V. Bogdanov [a,d], I.N. Flerov [a,c,*], N.M. Laptash [e]

[a] Kirensky Institute of Physics, Siberian Department of the Russian Academy of Sciences, 660036 Krasnoyarsk, Russia
[b] Astafijev Krasnoyarsk State Pedagogical University, 660049 Krasnoyarsk, Russia
[c] Institute of Engineering Physics and Radio Electronics, Siberian State University, 660074 Krasnoyarsk, Russia
[d] Krasnoyarsk State Agrarian University, 660049 Krasnoyarsk, Russia
[e] Institute of Chemistry, Far Eastern Department of the Russian Academy of Sciences, 690022 Vladivostok, Russia

ARTICLE INFO

Article history:
Received 7 December 2015
Received in revised form
1 February 2016
Accepted 17 February 2016
Available online 18 February 2016

Keywords:
Phase transition
Fluorides
Heat capacity
Entropy
Thermal expansion
High pressure

ABSTRACT

Calorimetric, dilatometric and differential thermal analysis studies were performed on $(NH_4)_3SnF_7$ for a wide range of temperatures and pressures. Large entropy ($\delta S_0 = 22$ J/mol K) and elastic deformation ($\delta(\Delta V/V)_0 = 0.89\%$) jumps have proven that the *Pa*-3 ↔ *Pm*-3*m* phase transition is a strong first order structural transformation. A total entropy change of $\Delta S_0 = 32.5$ J/mol K is characteristic for the order–disorder phase transition, and is equal to the sum of entropy changes in the related material, $(NH_4)_3TiF_7$, undergoing transformation between the two cubic phases through the intermediate phases. Hydrostatic pressure decreases the stability of the high temperature *Pm*-3*m* phase in $(NH_4)_3SnF_7$, contrary to $(NH_4)_3TiF_7$, characterised by a negative baric coefficient. The effect of experimental conditions on the chemical stability of $(NH_4)_3SnF_7$ was observed.

1. Introduction

A great interest of scientists and engineers to inorganic fluorides is owing to the possibility to design a huge number of materials with different crystal structures and with a diversity of useful physical chemical properties. Recently, many books and reviews were devoted to structures and functional properties of fluorinated compounds mainly at room temperature [1–7]. On the other hand, there exist rather wide families of fluorides changing significantly the symmetry of structure as the result of phase transitions under variation of temperature and/or pressure, which are also followed by strong change of many properties of different physical nature [8–10].

Although double fluoride salts with the general chemical formula of $A_3MeF_7 = A_3[MeF_6]F$ have long been known [11], it is only recently that they have been found to undergo structural phase transitions with a variety of distorted phase symmetries [12–14]. It was shown that depending on the size of the central Me atom, the transition between two cubic phases, *Pm*-3*m* and *Pa*-3, can be realised in a direct way in ammonium heptafluorostannate, $(NH_4)_3SnF_7$ [12], as well as through two intermediate ferroelastic tetragonal phases, *Pa*-3 ↔ *P*4/*mnc* ↔ 4/*m* ↔ *Pm*-3*m*, in ammonium heptafluorotitanate, $(NH_4)_3TiF_7$ [13–15].

At ambient pressure, the *Pm*-3*m* cubic phase in $(NH_4)_3TiF_7$ was not observed up to 380 K, where the crystal decomposed with the appearance of the $(NH_4)_2TiF_6$ phase [14]. This phenomenon has prevented the refining of the space group of the 4/*m* tetragonal phase in $(NH_4)_3TiF_7$ determined by polarizing optical observations [13]. However, the study of the susceptibility of this heptafluoride to hydrostatic pressure has revealed the triple point on the *T*–*p* phase diagram at $T_{trp1} = 345.5$ K and $p_{trp1} = 0.125$ GPa, in which the *P*4/*mnc*, 4/*m* and *Pm*-3*m* phases coexist. The extrapolation of the boundary between the *Pm*-3*m* and 4/*m* phases to p = 0 shows that the 4/*m* ↔ *Pm*-3*m* phase transition could take place at ambient pressure near a temperature of about 430 K, which exceeds the temperature of decomposition observed in X-ray studies. The second triple point, with coexistence of the *P*4/*mnc*, *Pa*-3 and *Pm*-3*m* phases, was also found on the *T*–*p* phase diagram of $(NH_4)_3TiF_7$ at $T_{trp2} = 298$ K and $p_{trp2} = 0.41$ GPa. Thus, the direct transformation between the two cubic phases, *Pm*-3*m* ↔ *Pa*-3, in heptafluorotitanate takes place upon cooling at $p > p_{trp2}$ [14].

The peculiarity of the $(NH_4)_3MeF_7$ compounds is that their structure can be considered in term of an $(NH_4)_3MeF_6$ network composed of MeF_6 octahedra interpenetrated with another network composed of "independent" F atoms linked to ammonium groups by N–H…F bonding. In Fig. 1, one can see the structure of the *Pm*-3*m* and *Pa*-3 cubic phases of heptafluorometallates, which are disordered and ordered, respectively [12–14].

$Me1F_6$ and $Me2F_6$ are octahedra oriented by different way in the low temperature cubic phase [12].

* Corresponding author at: Kirensky Institute of Physics, Siberian Department of the Russian Academy of Sciences, 660036 Krasnoyarsk, Russia.

http://dx.doi.org/10.1016/j.jssc.2016.02.027
0022-4596/

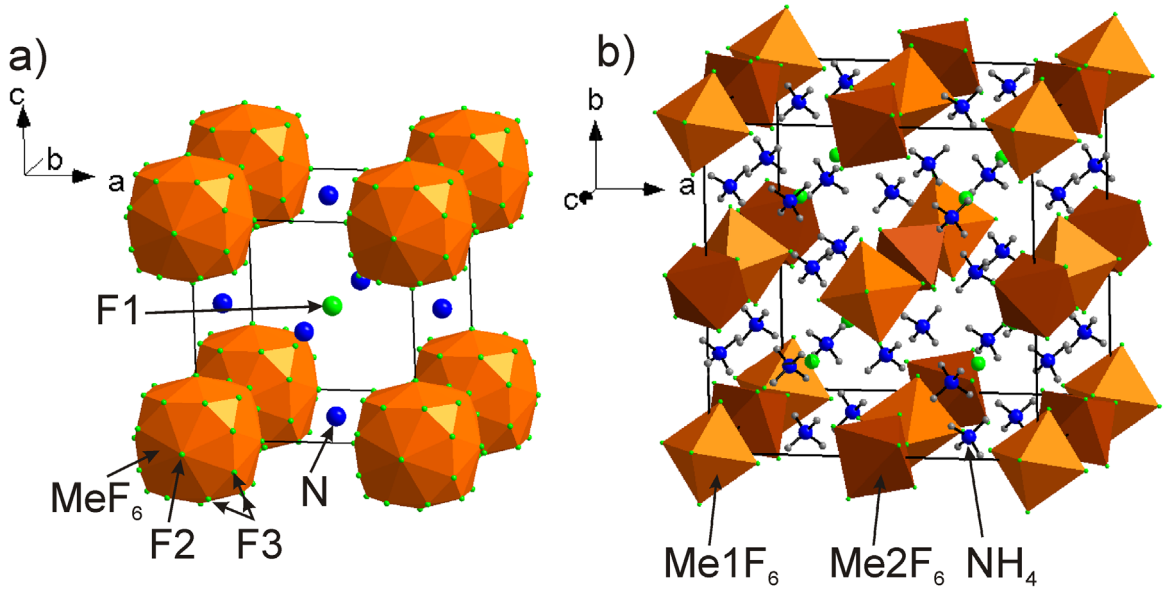

Fig. 1. Crystal structure of $(NH_4)_3MeF_7$: (a) *Pm*-3*m* and (b) *Pa*-3 phases. F1 – "independent" fluorine atom, F2 and F3 – fluorine atoms in 6*e* and 24*m* crystallographic sites, respectively.

In spite of hydrogen atoms were not located in the *Pm*-3*m* phase of $(NH_4)_3SnF_7$, tetrahedral cationic, $[NH_4]^+$, species were supposed to be disordered at least between two positions due to high 4/*mmm* symmetry of their crystallographic site (3*c*) [12]. Disorder of octahedral anionic, $[MeF_6]^{3-}$, groups between two sets of positions with different probabilities of occupation was also stated in the initial phase of ammonium heptafluorostannate [12]. Complete ordering of structural units, MeF_6 octahedra and NH_4 tetrahedra, was found in the low temperature *Pa*-3 cubic phase of $(NH_4)_3SnF_7$ as well as $(NH_4)_3TiF_7$ [12,14]. There are two nonequivalent MeF_6 octaherda with different orientations, $Me1F_6$ and $Me2F_6$, in this phase (Fig. 1b).

That is the successive and single phase transitions in $(NH_4)_3TiF_7$ and $(NH_4)_3SnF_7$, respectively, should be associated with the order–disorder processes. The results of calorimetric measurements on heptafluorotitanate have proven this supposition: large phase transition entropies exist at ambient as well as high pressure [15]. A preliminary study of heat capacity and thermal expansion performed on $(NH_4)_3SnF_7$ using differential scanning microcalorimetry (DSM) and X-ray diffraction (XRD), respectively, has also shown rather large entropy, ΔS, and unit cell volume, ΔV, changes for direct transformation between the two cubic phases [12]. Taking into account that these two experimental methods do not allow one to obtain exact information about the contributions from the pre-transitional heat and deformation effects into ΔS and ΔV at phase transitions, in this paper, we performed detailed investigations of the heat capacity and thermal dilatation of $(NH_4)_3SnF_7$ by means of sensitive methods such as adiabatic calorimetry and inductive dilatometry. The effect of hydrostatic pressure on the phase transition in heptafluorostannate was studied by experimental measurements of the baric coefficient using differential thermal analysis (DTA) and by evaluation of dT/dp from thermodynamic relations.

2. Experimental

The starting reagent for the synthesis of $(NH_4)_3SnF_7$ was metallic tin platelets (β-Sn) with 99.9% purity. Primarily, we tried to use the method of Plitzko and Meyer [16] which involves the oxidation of elemental Sn with NH_4HF_2:

$$Sn + 3.5NH_4HF_2 = (NH_4)_3SnF_7 + 0.5NH_3 + 2H_2,$$

however, the product yield due to this reaction carried out at ambient conditions was small (about 30%). So we used virtually complete tin dissolution in a mixture of pure nitric (56 mass % HNO_3) and hydrofluoric (40% HF) acids, for its oxidation and complexation in accordance with the reaction:

$$Sn + 6HF + 4HNO_3 = H_2SnF_6 + 4NO_2 + 4H_2O.$$

For example, 20 g of tin platelets were chemically etched in the excess of HF (60 ml) with the cautiously dropwise addition of HNO_3 (30 ml) at room temperature because of high exothermal character of the above reaction with the effervescence of brown NO_2. It took 15 min for complete dissolution of tin. The resulting solution pH was about 0, then $NH_3 \cdot aq$ (25%, 80 ml) was cautiously added to pH=4–5:

$$H_2SnF_6 + 2NH_3 = (NH_4)_2SnF_6.$$

The solution was evaporated on a water bath until the first appearance of crystals on the surface of the film solution. The final volume of solution was 70 ml. The first batch of crystals upon cooling to room temperature was 24 g (yield 53%). Thin hexagonal plates of $(NH_4)_2SnF_6$ were formed (the PXRD pattern were matching with the JCPDS file no. 026-0094), which were used for the synthesis of $(NH_4)_3SnF_7$. The large excess of NH_4F is needed relative to stoichiometry:

$$(NH_4)_2SnF_6 + NH_4F = (NH_4)_3SnF_7.$$

At least, a double excess of NH_4F relative to stoichiometry was used. For example, 10 g of $(NH_4)_2SnF_6$ were mixed with 4–4.5 g NH_4F in Pt or graphite glass cup and dissolved in 15 ml H_2O at heating on a water bath. The solution was evaporated until a crystalline film appearance on the surface of the solution. Upon cooling the solution to room temperature, a plentiful precipitate of colourless polyhedral crystals of $(NH_4)_3SnF_7$ was formed immediately, which was rinsed with ethanol under vacuum and air-dried. The yield was 8.3 g (73%). It took about 2 h to synthesize $(NH_4)_3SnF_7$.

The samples obtained were examined by XRD which revealed that at room temperature, cubic symmetry (sp. gr. *Pa*-3, $Z=8$) exists, consistent with the data of [12]. No additional phases were

observed in the sample.

Heat capacity measurements were performed in a wide temperature range of 82–364 K by means of a homemade adiabatic calorimeter with three screens, as described in [17]. The inaccuracy in the heat capacity determination did not exceed 0.5–1.0%. A "quasi-ceramic" sample in the form of a pressed pellet of 8 mm in diameter, 2 mm in height and with a mass of 0.189 g was prepared without heat treatment because of the presence of ammonium ions. The heat capacity of the "sample+heater+contact grease" system was measured using discrete as well as continuous heating. In the former case, the calorimetric step was varied from 1.5 to 3.0 K. In the latter case, the system was heated at rates of $dT/dt \approx 0.15$–0.30 K/min. The heat capacities of the heater and contact grease were determined in individual experiments.

Thermal dilatation of the sample examined in calorimetric measurements was studied in a temperature range of 100–425 K with a heating rate of 3 K/min using a NETZSCH model DIL-402C pushrod dilatometer. In order to remove the influence of thermal expansion in the system, calibration of the results was carried out with quartz as the standard reference.

The effect of hydrostatic pressure on the temperature and enthalpy of the *Pa*-3↔*Pm*-3*m* phase transition was experimentally studied by DTA. A copper container with a powder sample of 0.05 g and the reference quartz sample were glued onto opposite junctions of a highly sensitive (~100 μV/K) germanium-copper thermocouple. This system was placed inside a piston-cylinder type vessel which was associated with a pressure multiplier. Silicon oil was used as the pressure-transmitting medium. Because of the rather high phase transition temperature, pressure measurements were carried out only up to 0.2 GPa.

3. Results and discussion

The previous XRD study [12] showed that the *Pa*-3↔*Pm*-3*m* phase transition (~360 K) and decomposition (~370 K) temperatures in $(NH_4)_3SnF_7$ are close. Taking into account this fact and the much lower pressure used in calorimetric investigations (10^{-5} mm Hg) compared to structural experiments (10^{-2} mm Hg), one could suppose that during the heat capacity measurements, $(NH_4)_3SnF_7$ could start to decompose at lower temperatures. The appearance of even a small amount of $(NH_4)_2SnF_6$ in the $(NH_4)_3SnF_7$ sample could reliably be detected owing to the large enthalpy (entropy) change at the structural transformation near 110 K, found recently by us in $(NH_4)_2SnF_6$ [18].

In Fig. 2, one can see the results of the specific heat measurements on $(NH_4)_3SnF_7$ obtained in three successive experiments with an adiabatic calorimeter. In the first heating, the anomalous behaviour of the heat capacity was found only in the region of the *Pa*-3↔*Pm*-3*m* phase transition at 356 K (Fig. 2a). The second series of measurements demonstrated the appearance of an additional heat capacity peak at 107.3 K, associated with the phase transition in the $(NH_4)_2SnF_6$ compound which appeared in the sample during the first heating process up to 359.2 K only (Fig. 2b). In the third heating, the heat capacity anomaly from $(NH_4)_2SnF_6$ increased and shifted to a higher temperature of 108.6 K. Thermal cycling was accompanied by a small change in the phase transition temperature in the $(NH_4)_3SnF_7$ sample, $T_0 = 356 \pm 1$ K. Simultaneously, the enthalpy change at T_0 decreased in accordance with the increasing amount of $(NH_4)_2SnF_6$ in the sample under investigation.

The entropy of the phase transition in $(NH_4)_3SnF_7$ was determined by integration of the excess heat capacity, $\Delta S_0 = \int(\Delta C_p/T)dT$, obtained from the analysis of the first series data when the sample was free of the $(NH_4)_2SnF_6$ impurity. The $\Delta C_p(T)$ dependence was obtained from the difference between the

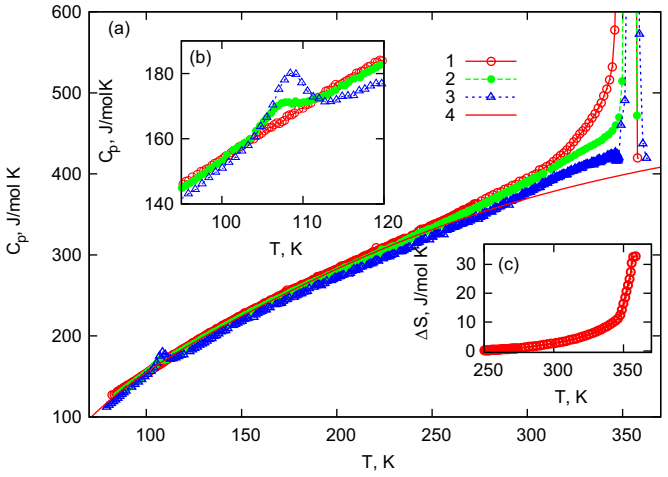

Fig. 2. (a) Temperature dependence of the heat capacity obtained in the first (1), second (2) and. third (3) series of measurements on $(NH_4)_3SnF_7$. Lattice heat capacity is shown by the solid line (4). (b) Behaviour of $C_p(T)$ in the temperature region of structural transformation near 110 K in the $(NH_4)_2SnF_6$ phase, which appeared in the sample after heating above temperature of phase transition in $(NH_4)_3SnF_7$. (c) Temperature dependence of the excess entropy of $(NH_4)_3SnF_7$.

total experimentally found C_p and lattice C_{lat} heat capacities. The $C_{lat}(T)$ contribution was determined by the approximation of the experimental data using equation $C_{lat} = a + bT + cT^{-2} - dT^2$. In Fig. 2a, C_{lat} is presented as a dashed line.

Fig. 2c shows that excess entropy exists in a very wide temperature range for the *Pa*-3 phase, almost down to 200 K. This is the reason for very large entropy change, $\Delta S_0 = 32.5 \pm 2.5$ J/mol K, which strongly exceeds the entropy determined by DSM experiments, which are not sensitive to pre-transitional heat effects [12]. This ΔS_0 value is characteristic for the direct transformation between two cubic phases in $(NH_4)_3SnF_7$ and is in a good agreement with the total entropy change, $\Sigma\Delta S_i = 33.5 \pm 3.5$ J/mol K, associated with three successive phase transitions, *Pa*-3↔*P*4/*mnc*↔4/*m*↔*Pm*-3*m*, in the related $(NH_4)_3TiF_7$ compound [15]. Such a large value for the phase transition entropy shows, unambiguously, that structural distortions in both heptafluorides are connected with some order–disorder processes. Indeed, the structural analysis has revealed that all structural elements are ordered in the *Pa*-3 phase, while octahedral $Sn(Ti)F_6$ and tetrahedral NH_4 groups are significantly disordered in the *Pm*-3*m* of $(NH_4)_3SnF_7$ and intermediate tetragonal *P*4/*mnc* and 4/*m* phases of $(NH_4)_3TiF_7$ [12,14].

In accordance with structural model, three NH_4 tetrahedra are orientationally disordered between two positions in the *Pm*-3*m* phase of $(NH_4)_3SnF_7$ [12]. Disorder of SnF_6 species is rather complicated because each octahedron has one and four orientations with the probabilities of 1/2 and 1/8, respectively (Fig. 1a). The first orientation is consistent with the ordered octahedron in the *Pm*-3*m* and *Pa*-3 phases. Thus, the phase transition *Pm*-3*m*↔*Pa*-3 is associated with the ordering of the second set of orientations. In the case of the total ordering of structural elements in *Pa*-3 phase postulated in [12], the rough estimation of the entropy associated with the structural transformation leads to the value $\Delta S_0 = 3R\ln 2 + 1/2R\ln 4 = 23.1$ J/mol K, which is significantly less than the experimentally found entropy. The reason of this difference is that the structural distortions in the *Pa*-3 phase are associated not only with the ordering of tetrahedra and octahedra but also with breaking of hydrogen bonds, huge rotations of ordered octahedra and large displacements of the F ions, which give additional contribution to the entropy change (Fig. 1b, [12,14]).

The temperature dependences of the linear deformation, $\Delta L/L$, as well as the coefficient of thermal linear expansion, α, are shown in Fig. 3. The first heating in a temperature range of 100–380 K

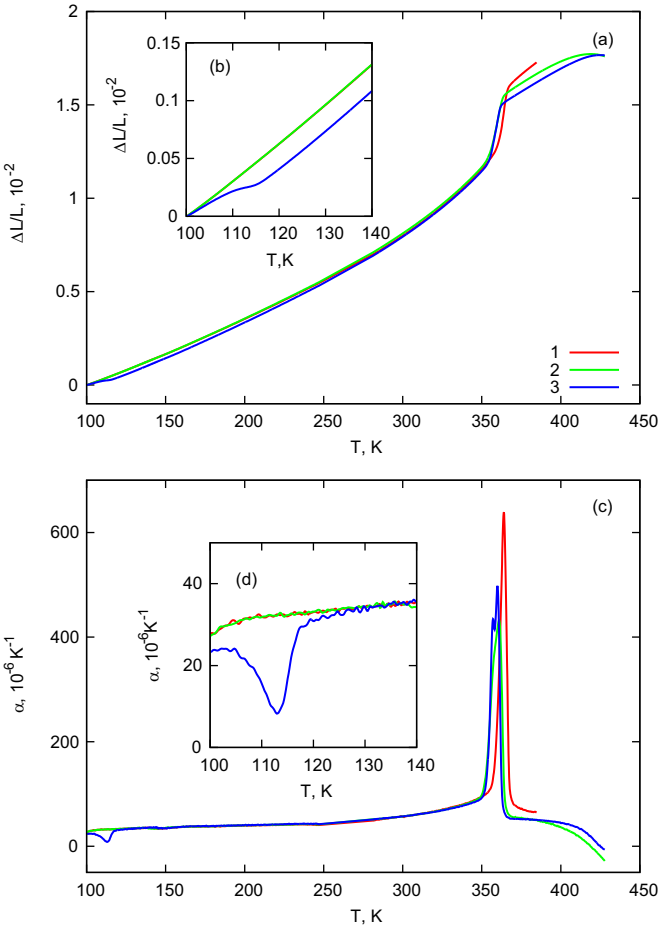

Fig. 3. Temperature dependence of (a) strain and (c) the thermal expansion coefficient of $(NH_4)_3SnF_7$ obtained in three series of measurements. (b, d) Anomalous behaviour of both values at the phase transition in $(NH_4)_2SnF_6$, which appeared after the second series of measurements.

revealed that both properties demonstrated strong anomalous behaviour associated with the *Pa*-3 ↔ *Pm*-3*m* phase transition in $(NH_4)_3SnF_7$ at 364 K. The second and third series of measurements performed up to 430 K showed a rather strong decrease in α above 380 K, as well as a decrease in the phase transition temperature down to 361 and 360 K, respectively (Fig. 3c). Here one can also see the splitting of the α anomaly near 360 K after the first heating the sample up to 380 K. The $(NH_4)_2SnF_6$ phase as decomposition product does not undergo structural transformation in this temperature region. One can suppose that decomposition process is followed by the appearance of inhomogeneity of the sample, which leads to different temperatures of phase transition in different parts of the $(NH_4)_3SnF_7$ sample.

Moreover, Fig. 3a demonstrates a small decrease in the $\Delta L/L$ jump at T_0 in these experiments. The volume change in the region of the phase transition is about $\delta(\Delta V/V)_0 = 8.9 \cdot 10^3$.

As for the heat capacity, the contribution of the pre-transitional anomalous effects to thermal dilatation was also observed for a wide temperature region below T_0.

The appearance of the $(NH_4)_2SnF_6$ phase was detected only in the third series of measurements, where the anomaly of thermal dilatation was also observed at 113 K, which is close to the temperature of the phase transition in pure hexafluorostannate [18] (Fig. 3b and d).

The results obtained have shown that in dilatometric experiments, the chemical stability of $(NH_4)_3SnF_7$ was maintained up to much higher temperatures in comparison with XRD studies [12] and calorimetric measurements. The reason for this is that thermal dilatation was studied under different conditions, namely, in a helium medium under pressure of about 10^5 Pa, which prevented the decomposition of $(NH_4)_3SnF_7$.

Fig. 4a depicts the typical behaviour of the DTA signal at different pressures in the region of the *Pa*-3 ↔ *Pm*-3*m* phase transition in $(NH_4)_3SnF_7$. As the temperature dependence of the anomalous DTA signal is proportional to the temperature dependence of the anomalous heat capacity, $\Delta C_P(T)$, the area under the DTA peak is proportional to the enthalpy of the phase transition. All the DTA peaks are practically symmetric and exist in a narrow temperature range of 5–7 K (Fig. 4a). This means that only the enthalpy jump (latent heat), δH_0, was observed in the DTA measurements. Under pressure, the DTA peaks were shifted to a higher temperature and slightly broadened at almost constant maximum values, which means that a small increase in δH_0 has occurred. Thus, one can suggest that the entropy jump at the phase transition, $\delta S_0 = \delta H_0 / T_0$, remained constant, at least for the pressure range studied.

The pressure–temperature phase diagram of $(NH_4)_3SnF_7$ is shown in Fig. 4b. The boundary between the two cubic phases is practically linear and can be described adequately with the baric coefficient, $dT_0/dp = 47 \pm 4$ K/GPa.

The susceptibility of the first order phase transition to hydrostatic pressure can also be evaluated in the framework of the Clausius–Clapeyron equation, $dT_0/dp = \delta V_0/\delta S_0$, using the heat capacity and thermal dilatation data. The values of the entropy and volume jumps at the phase transition point were determined as $\delta S_0 = 22$ J/mol K and $\delta V_0 = 2$ Å^3, respectively. The calculated baric coefficient, $dT_0/dp = 54$ K/GPa, is in a good agreement with the experimentally determined value. This fact unambiguously shows the reliability of the information about thermal properties obtained by the three independent experimental methods.

It should be noted that there is an intriguing feature associated with the different signs of the baric coefficient for the boundary between *Pa*-3 and *Pm*-3*m* phases in $(NH_4)_3TiF_7$ ($dT_0/dp = -40$ K/GPa) [15] and $(NH_4)_3SnF_7$. As the entropy always increases with increasing temperature, in accordance with the Clausius–Clapeyron equation, the observed difference is due to the different sign of the unit cell volume change for the phase transition. It is difficult to provide a strong explanation for this discrepancy. However, one can think that the reason is connected to the different pressure and temperature conditions at which the *Pa*-3 ↔ *Pm*-3*m* phase transition is realised in both ammonium heptafluorides. In $(NH_4)_3TiF_7$, the direct transformation between the two cubic phases was found for pressures above 0.41 GPa and temperatures below 300 K [15]. Thus, the small unit cell volume of $(NH_4)_3TiF_7$ compared to $(NH_4)_3SnF_7$ is additionally decreased in the region of the *Pa*-3 ↔ *Pm*-3*m* transformation by hydrostatic pressure and low temperature. In such a case, one can tentatively suggest that in the $(NH_4)_3$[Sn–Ti]F_7 solid solutions, the baric coefficient may change sign with an increase in titanium concentration.

4. Conclusions

In the present paper, we continued to investigate the peculiarities of the thermal properties in double fluoride salts, $A_3MeF_7 = A_3[MeF_6]F$.

Strong first order behaviour for the *Pa*-3 ↔ *Pm*-3*m* transformation in $(NH_4)_3SnF_7$ was proven by large entropy, $\delta S_0 = 22$ J/mol K, and volume, $\delta(\Delta V/V)_0 = 0.89\%$, jumps at the phase transition point. The anomalous behaviour of the heat capacity and thermal dilatation was found for a wide temperature range from T_0 down to 200 K, leading to a significant total change in both the entropy, $\Delta S_0 = 32.5$ J/mol · K, and unit cell volume, $\Delta V_0 = 3.1$ Å^3.

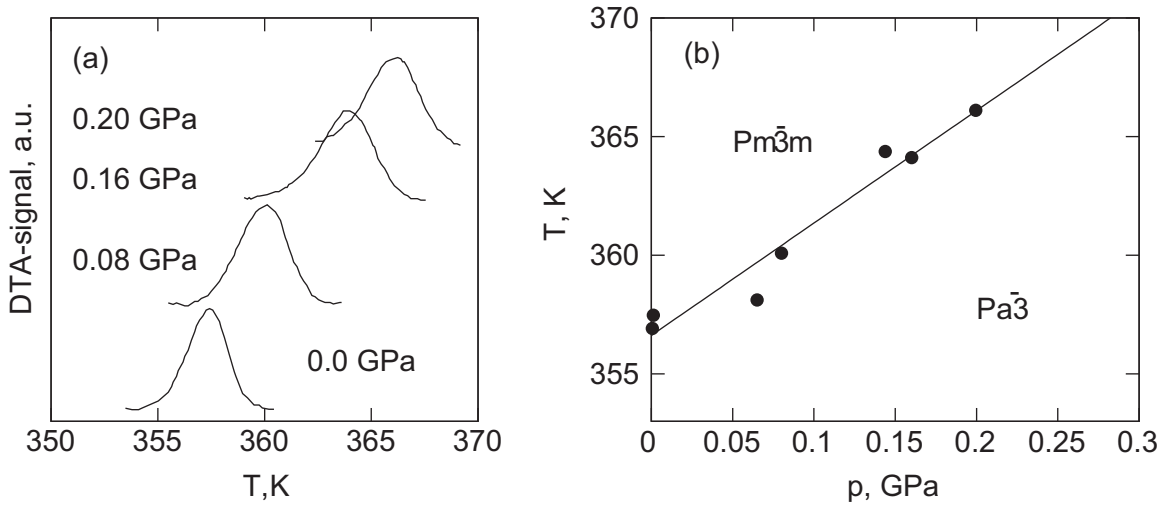

Fig. 4. (a) Behaviour of the DTA signal against temperature and pressure and (b) the temperature–pressure phase diagram of $(NH_4)_3SnF_7$.

Large experimentally found entropy exceeds the value followed from the model associated only with the complete ordering of all structural units below T_0 because, as it was shown in [12], there are additional structural distortions giving contribution to the ΔS_0 value. On the other hand, ΔS_0 in $(NH_4)_3SnF_7$ at the direct *Pa*-3 ↔ *Pm*-3*m* phase transition is close to the sum of entropy changes associated with the successive transformations of *Pa*-3 ↔ *P*4/*mnc* ↔ 4/*m* ↔ *Pm*-3*m* in $(NH_4)_3TiF_7$ [15].

The study of the hydrostatic pressure effect on the phase transition in $(NH_4)_3SnF_7$ revealed the constancy of the entropy change and increase of phase transformation temperature.

In order to explain the different signs of the baric coefficient for the *Pa*-3 ↔ *Pm*-3*m* phase transition in ammonium heptafluorides with Sn and Ti as the central atoms, a study of $(NH_4)_3$[Sn–Ti]F_7 solid solutions is needed.

It was found that the temperature of $(NH_4)_3SnF_7$ decomposition accompanied by the appearance of $(NH_4)_2SnF_6$ phase strongly depends on the experimental pressure.

Acknowledgements

This study was partially supported by the Russian Foundation for Basic Research (RFBR), research Project no. 15-02-02009a.

References

[1] J.S. Thrasher, S.H. Strauss, Inorganic Fluorine Chemistry: Toward the 21st Century. ACS Symposium Series 555, American Chemical Society, Washington, DC, 1994.
[2] T. Nakajima, B. Zemva, A. Tressaud, Advanced Inorganic Fluorides, Elsevier, Amsterdam, 2000.
[3] T. Nakajima, H. Groult, Fluorinated Materials for Energy Storage, Elsevier, Amsterdam, 2005.
[4] A. Tressaud, Functionalized Inorganic Fluorides, Wiley-Blackwell, Chichester, 2010.
[5] E.V. Antipov, A.M. Abakumov, Synthesis, structure and superconducting/magnetic properties of Cu- and Mn-based oxyfluorides, in: A. Tressaud (Ed.), Functionalized Inorganic Fluorides, Wiley-Blackwell, Chichester, 2010, pp. 383–422.
[6] M. Leblanc, V. Maisonneuve, A. Tressaud, Crystal chemistry and selected physical properties of inorganic fluorides and oxide–fluorides, Chem. Rev. 115 (2015) 1191–1254.
[7] R. Gautier, K.B. Chang, K.R. Poeppelmeier, On the origin of the differences in structure directing properties of polar metal oxyfluoride $[MO_xF_{6-x}]^{2-}$ ($x=1, 2$) building units, Inorg. Chem. 54 (2015) 1712–1719.
[8] I. Flerov, M. Gorev, K. Aleksandrov, A. Tressaud, J. Grannec, M. Couzi, Phase transitions in elpasolites (ordered perovskites), Mater. Sci. Eng. R-Rep. 24 (1998) 81–151.
[9] J. Ravez, Ferroelectricity in solid state chemistry, C. R. Acad. Sci. Paris. Ser. IIc, Chim./Chem. 3 (2000) 267–283.
[10] J.F. Scott, R. Blinc, Multiferroic magnetoelectric fluorides: why are there so many magnetic ferroelectrics? J. Phys.: Condens. Matter 23 (113202) (2011) 17pp.
[11] J.L. Hoard, M.B. Williams, Structures of complex fluorides. ammonium hexafluosilicate—ammonium fluoride, $(NH_4)_2SiF_6 \cdot NH_4F$, J. Am. Soc. 64 (1942) 633–637.
[12] I.N. Flerov, M.S. Molokeev, N.M. Laptash, A.A. Udovenko, E.I. Pogoreltsev, S. V. Mel'nikova, S.V. Misyul, Structural transformation between two cubic phases of $(NH_4)_3SnF_7$, J. Fluor. Chem. 178 (2015) 86–92.
[13] S.V. Mel'nikova, E.I. Pogoreltsev, I.N. Flerov, N.M. Laptash, Unusual sequence of phase transitions in $(NH_4)_3TiF_7$ detected by optic and calorimetric studies, J. Fluor. Chem. 165 (2014) 14–19.
[14] M.S. Molokeev, S.V. Misjul, I.N. Flerov, N.M. Laptash, Reconstructive phase transition in $(NH_4)_3TiF_7$ accompanied by the ordering of TiF_6 octahedra, Acta Cryst. B70 (2014) 924–931.
[15] E.I. Pogoreltsev, I.N. Flerov, A.V. Kartashev, E.V. Bogdanov, N.M. Laptash, Heat capacity, entropy, dielectric properties and *T*–*p* phase diagram of $(NH_4)_3TiF_7$, J. Fluor. Chem. 168 (2014) 247–250.
[16] C. Plitzko, G. Meyer, Kristallstruktur von $(NH_4)_3SnF_7$: Ein doppelsalz gemäß $(NH_4)_3[SnF_6]F$ und kein $(NH_4)_4SnF_8$, Z. Anorg. Allg. Chem. 623 (1997) 1347–1348.
[17] A.V. Kartashev, I.N. Flerov, N.V. Volkov, K.A. Sablina, Adiabatic calorimetric study of the intense magnetocaloric effect and the heat capacity of $(La_{0.4}Eu_{0.6})_{0.7}Pb_{0.3}MnO_3$, Phys. Solid State 50 (2008) 2115–2120.
[18] I.N. Flerov, A.V. Kartashev, M.V. Gorev, E.V. Bogdanov, S.V. Mel'nikova, M. S. Molokeev, E.I. Pogoreltsev, N.M. Laptash, Thermal, structural, optical, dielectric and barocaloric properties at ferroelastic phase transition in trigonal $(NH_4)_2SnF_6$: a new look at the old compound, J. Fluor. Chem. 183 (2016) 1–9.